Journal of Structural Geology, Vol. 8, No. 1, pp. 87 to 100, 1986
Printed in Great Britain

0191-8141/86 $03.00 + 0.00

Orthographic analysis of geological structures—II. Practical applications

DECLAN G. DE PAOR

Department of Earth & Planetary Sciences, The Johns Hopkins University, Baltimore, MD 21218, U.S.A.

(*Received* 21 *April* 1985; *accepted in revised form* 11 *July* 1985)

Abstract—The deformation suffered by an object is directly related to the angle of inclination required to interpret its outline as an oblique view of an undeformed object. This relationship is the basis of orthographic strain analysis, the continuum mechanical theory of which was discussed in Part I. Part II comprises step-by-step instructions for determining strain from a wide variety of markers, for restoring the three-dimensional strain configuration from two-dimensional data and for incorporating strain data in structural sections.

INTRODUCTION

SINCE the pioneering work of Cloos (1947) structural geologists have been aware of the important role that strain studies can play in a regional tectonic synthesis. However, while deformation theory has received much attention (Flinn 1962, Ramsay 1967, Means 1976), practical applications in the scale of Cloos (1971) are rare. A great deal of time and energy has been expended on discussions, or disputes, about theory. In contrast, few structural geologists regularly incorporate strain data in their structural sections in the style of Hossack (1978) and even fewer deduce from three oriented sectional ellipses the principal stretch ratios and axial orientations of the deformation ellipsoid. Yet this latter is a necessary first step in rendering strain data relevant to tectonics. An isolated strain reading is as sterile as a radiometric date from a loose boulder! Stripped of structural setting and field relations, knowledge that the stretch ratio R_s = 2.5 prompts the question "so what"? What matter most are (i) the strain trajectories, which may reveal whether a tectonic regime is purely compressional, or a complex wrench type, for example, and (ii) outcrop or map-scale strain-intensity variations, which may reveal a lot about deformation mechanisms and the temporal evolution of structures.

Part I of this paper (De Paor 1983) dealt with the theory of orthographic analysis of geological structures. Here I will tackle the problem of using strain analysis in practice. In the following practical applications, I bear in mind the ultimate goals of specifying the three-dimensional strain rate and incorporating homogeneous strain data in heterogeneously deformed structural sections. The techniques described employ simple constructions on the orthonet and can often be used on location in the field.

The *orthographic net*, or orthonet (De Paor 1983, fig. 1), is a projection of the meridians and parallels of a unit sphere onto a plane such that all projection lines are parallel to each other and perpendicular to the plane (Fig. 1). A point with coordinates (l, m, n) on the sphere becomes (l, m) on the projection. A plunge of ϕ is represented by a point Cos ϕ from the centre pin and a plane of dip δ is represented by an elliptical great circle of unit long axis and short axis Cos δ, one side of the long axis representing upper hemisphere projection, the other lower. Fundamental to the techniques which follow is the ability to view a great circle in two ways: as a spatial view of a true circle inclined at an angle δ and as a normal view of an ellipse of axial ratio 1/Cos δ, lying in the plane of the diagram.

Traditionally, orientation nets in structural geology represent directions in a geographical reference frame such as north-east-down. To understand the orthographic analysis of geological structures, one must be prepared to abandon these conventions. The orthonet conserves vector operations of addition and factorization and is used to represent magnitudes and orientations. Furthermore, the reference frame will often be chosen to coincide with structural features, regardless of their geographic orientations. Reference frames may be classified according to structural setting, as follows:

(i) *Compaction related*

For this type of deformation, the principal directions are vertical and horizontal and there is no active rotation

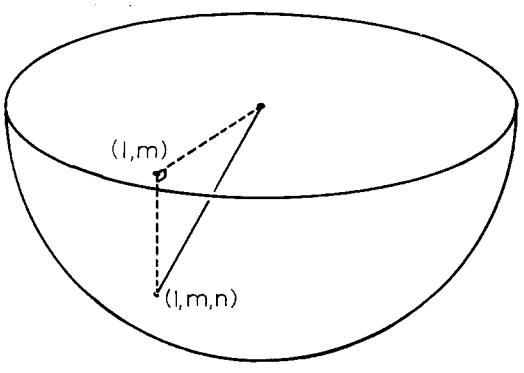

Fig. 1. Orthographic projection maps the point (l, m, n) on the unit sphere into the point (l, m) on the projection plane. All lines of projection are parallel to each other and perpendicular to the projection plane.

or horizontal extension. Only one variable remains; it may be expressed as a vertical stretch S, a longitudinal strain $e = S - 1$ or as a volume change $\Delta V = e$. Because only one variable is sought, little evidence is required and a wide variety of strain markers is possible.

(ii) *Cleavage related*

In many cases, cleavage may be assumed to lie close to a principal plane of the strain ellipsoid (strictly speaking, this is the left stretch ellipsoid, the irrotational component of deformation in its final orientation but one may use the casual term 'strain ellipsoid' when such strict specification is not critical). Often an associated mineral lineation locates the principal directions in the plane of cleavage. Because the axis of a sectional ellipse does not have to lie in a principal plane of its parent ellipsoid, it is not valid to align a section's maximal stretch direction with the trace of cleavage unless the section plane contains the pole to cleavage (see Sanderson 1974). It is common practice to cut one section perpendicular and a second parallel to the mineral elongation in the cleavage plane (otherwise a third section is required to fully determine the three dimensional strain state. These sections can be, but need not be, mutually perpendicular). Two variables are sought, the principal stretch ratios R_{xy} and R_{yz} (plus a third, the pitch of the maximal stretch in the absence of a lineation); therefore the range of sufficient strain data sets is more limited. Rotational contributions to deformation cannot be detected.

(iii) *Shear-zone related*

Complexities increase if one chooses the pole to a planar shear-zone as one reference axis, the other two being either oriented arbitrarily or parallel and perpendicular to the displacement direction. Correspondingly, the rewards of such analyses are greater, since one may determine both the stretch and rotational components of deformation. Given sufficient data, useful information may be extracted even from zones of superposed pure and simple shear in a predeformed host.

(iv) *Arbitrarily oriented*

For arbitrary geographical reference frames the variables are most numerous and the data requirements correspondingly large. It is generally impossible to infer the rotational component of deformation, even when palaeo-plumblines or palaeo-spiritlevels are available (for example, the dip of beds that were initially horizontal is of little value, since the material aligned along the final dip direction may have changed trend). Five variables must be specified, namely the principal stretch ratios R_{xy}, R_{yz} and three Euler angles of the left principal stretch directions.

In each of these settings possible strain markers may be classified as follows:

(i) *Angular strain markers.* They record the change in an angle of known initial value. Examples include many fossils where the initial angular relations are well constrained by pristine individuals, bedforms such as cross strata where initial angular relations are less precise, and planes such as lithological contacts that are traced in the field from undeformed wall rock into deformed zones.

(ii) *Longitudinal strain markers.* They record changes in lengths of lines. Examples include belemnites, tourmalines and rutiles, which respond to applied stress in a brittle fashion, developing locally heterogeneous strain fields, but which are themselves of insignificant volume and thus serve to gauge the longitudinal strain that the host would have suffered in their absence.

(iii) *Fabric elements.* These are semi-quantitative indicators of incremental or cumulative strain. Examples include fibres, stylolites and crystallographic axes. They are not amenable to orthographic analysis but may be combined with quantitative strain markers to great effect.

(iv) *Deformed object distributions.* Here the magnitudes of individual lengths or angles are not known but statistical distributions are modelled as either initially random, uniform, anticlustered or symmetrical about a known direction. The effects of deformation upon distribution statistics permit strain computations. Fry (1979) used anti-clustered point distributions and De Paor (1979a, 1981a, b, c) introduced the orthographic strain analysis of line distributions. Therefore this class of strain markers are not further discussed here.

(v) *Rational markers.* These are sufficient alone to determine strain ratios. Examples include angular strain rosettes such as *Pentacrinus* ossicles and many fossils with landmarks of known initial relative orientation and separation.

(vi) *Whole deformation markers.* These are sufficient alone to determine both the rotational and stretch components of deformation. A simple example is the trace of cleavage in a zone of simple shear cutting undeformed host-rock. A particularly attractive marker was recently discovered by Ford & Ferguson (1985). It consists of a twinned arsenopyrite crystal of initial hexagonal symmetry, with elongate prisms radiating at initial 60° intervals. Each arm of the deformed crystals suffered boudinage as well as angular strain, and fibrous growths between boudins constrain the possible incremental rotations. Such whole-deformation markers are devoutly to be sought!

The six marker types defined above could be analyzed in each of the previously enumerated reference frames. However, to avoid duplication, such comprehensive coverage is curtailed. To begin with an easily visualized example, consider the coin superimposed on an orthonet

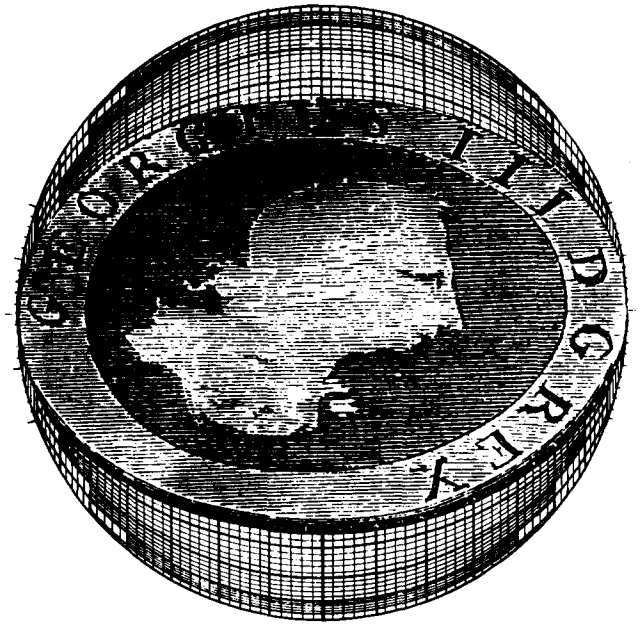

Fig. 2. Image of a coin superimposed on an orthonet (see Daubrée 1879, fig. 156). The human eye cannot tell whether the coin is deformed or merely inclined to the line of sight.

ANGULAR STRAIN MARKERS

I begin with the case of compaction (Exercises 1–3) because the constructions are simplest when there is no horizontal extension. Having advanced to more complicated cases, the interested reader may return to the examples used for compaction and very simply modify them to render them more generally applicable.

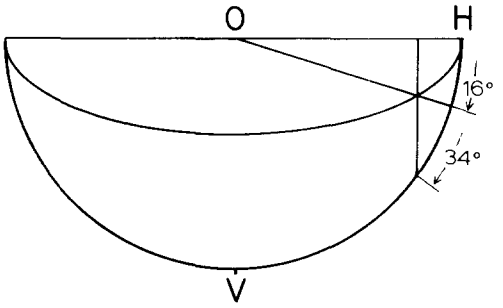

Fig. 3. Orthographic analysis of compacted cross stratification. The radius of the net is drawn at 16° to the horizontal (H). V represented the vertical. The small circle is drawn at 34° from H. this being the assumed initial foreset dip. The great circle represents the strain ellipse.

in Fig. 2. Familiarity with circular coins leads the eye to interpret this as an undeformed object oriented at an angle of 45° to the paper. In fact the coin was deformed by Daubrée (1879, fig. 156); it is truly elliptical, with an axial ratio of 1.4, a figure close to the secant of 45°.

It is not necessary for the field geologist to be familiar with a host of mathematical formulae for different kinds of strain marker. All rational markers obey the following simple rule: *The axial ratio of the deformation ellipse is the secant of the angle through which one must tilt one's line of sight in order to make the object appear undeformed, and the long axis lies in the direction towards which one must tilt.* (A secant is used to describe the forward deformation because the foreshortening, or undeforming, effect of an oblique view obeys a cosine law; the long axis of the forward deformation lies in the direction of tilt because that direction is most foreshortened, i.e. most effectively undeformed, in the oblique view. One is assumed to view the object orthographically, as if through a telephoto lens.) Thus the problem of determining the stretch ratio R_s can be solved using the equation

$$R_s = \text{Sec } \delta, \qquad (1)$$

if one knows the 'view angle' δ. δ may be estimated by eye in the field but errors are likely to be large. A more satisfactory approach is to use the orthonet to determine the inclination of the plane in which the object could be thought to lie undeformed. Angular and longitudinal strain markers may also have their initial dimensions restored by oblique viewing, but given only one such marker there are many possible directions of tilting, each with its associated angle δ.

A series of exercises in orthographic strain analysis follows.

Exercise 1: To determine the amount of compaction suffered by cross strata (Fig. 3)

Given the post-compactional dip of cross strata in a horizontal bed, one may determine the amount of vertical shortening assuming an acceptable initial foreset dip. Borradaile (1973) cited 24–44° as the range in undeformed sub-aerial deposits. For a post-compaction dip of 16°, proceed as follows.

(i) Position the net with its axis horizontal and label the reference frame as in Fig. 3. Plot the foreset strike at the centre pin and, on an overlay, trace a radial line at 16° to the horizontal. This is the foreset trace.

(ii) Select an acceptable initial foreset dip from the above range, say 34°. Counting out from the axis, note the 34° small circle's point of intersection with the forset trace. The great circle which passes through this intersection point is the required compaction ellipse.

(iii) Modify the assumed initial foreset dip, repeat the analysis and note the effect upon the calculated compaction.

This exercise clearly illustrates the need to switch from a conventional view of the net, in which two great circles and a small circle are seen to intersect at a point, to a two-dimensional view in which the radius represents the foreset dip-line, the vertical line represents a displacement path and the ellipse represents the compacted equivalent of the primitive circle.

Exercise 2: To determine the amount of compaction suffered by a floral stem

Consider a floral stem fragment furrowed along its length and jointed initially at right angles to the furrows (Fig. 4a).

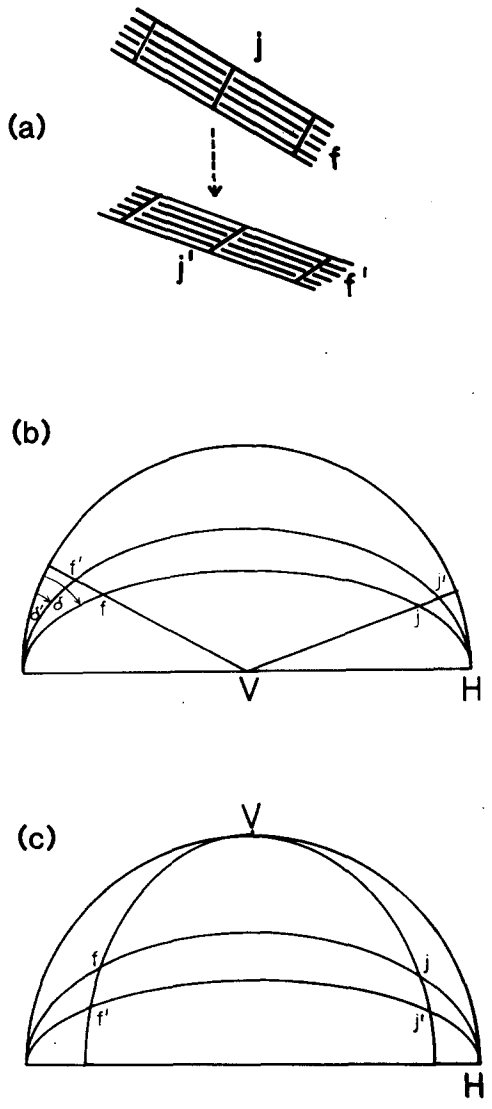

Fig. 4. Orthographic construction for a deformed floral stem shown in (a). The reference frame in (b) is conventional (horizon represented by the perimeter); in (c) the perimeter contains vertical and horizontal lines, V and H. f and j are the initial furrow and joint directions (they subtend an angle of 90° when viewed perpendicular to the fossil plane as in (a); f' and j' are the deformed equivalents. δ and δ' are the initial and final dips of the fossil plane. See text.

(i) Using the net in a conventional way (Fig. 4b), trace the plane of the fossil and on it mark points f' and j' pitching parallel to the deformed furrows and joints.

(ii) Join f' and j' to the centre. These radial great circles are the trajectories of the furrow and joint orientations during compaction.

(iii) Find the steeper dipping great circle which intersects the trajectories in points f and j pitching 90° apart. This great circle represents the undeformed fossil plane. In it the single geometric criterion of initial furrow-joint perpendicularity is met.

(iv) Measure the initial and final fossil plane dips, δ and δ', and use Sorby's formula,

$$\text{Tan } \delta = R_s * \text{Tan } \delta' \qquad (2)$$

to determine the compaction ratio R_s. Depending on the fossil orientation, the reference frame of Fig. 4(c) may be preferred.

Exercise 3: To determine the amount of compaction suffered by an unoriented ammonite

Sanderson (1976) described a case where compaction can be evaluated from a deformed ammonite. The fossil's spiral section is analysed using the method of Tan (1973). This gives an elliptical section of the compaction ellipsoid; unfortunately, the section's field orientation is unknown. The geometry of compaction implies that the ellipse's long axis was horizontal and did not suffer any change in length.

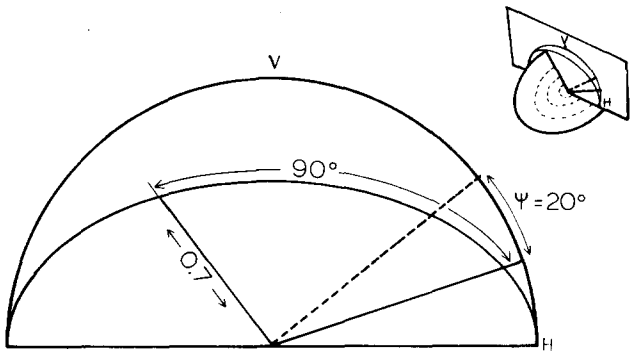

Fig. 5. Strain analysis using a compacted ammonite. 20° is the angular shear of the fossil's central axis; 0.7 is the stretch of its short axis. The overlay is rotated until a 90° pitch is subtended between them.

(i) Plot that axis at the centre pin of Fig. 5.

(ii) Let the short axis stretch be 0.7 and the deflection of the cylinder axis from orthogonality be 20°. Draw any radial line of 0.7 units length (either side of the pin) to represent the ellipse's short axis and draw a second radial line of arbitrary length, deflected 20° from perpendicularity to the first, representing the deformed cylinder axis.

(iii) Rotate the tracing paper until a horizontal great circle passes through the tip of the short axis and simultaneously subtends a pitch angle of 90° between short axis and cylinder axis. This great circle is the compaction ellipse.

Exercise 4: Pure shear of bilaterally symmetrical fossils

Determining the two dimensional deformation of trilobites, brachiopods and other bilaterally symmetrical forms is a simple matter if the fossils lie in bedding, and cleavage is developed perpendicular to the plane of bedding.

(i) Make tickmarks on an overlay to represent the trace of cleavage and rotate the axis of the net into alignment with the tickmarks. Trace the deformed lines of fossil symmetry in the correct relative directions (Fig. 6a).

(ii) Inspect the great circles of the net until one is found to be divided into four 90° quadrants by the symmetry lines (be sure to measure angles as pitches, along the great circle). The chosen great circle has an axial ratio (secant of dip) equal to the stretch ratio R_s.

In the absence of a cleavage trace, one fossil does not suffice, for a different ratio R_s can be calculated for each

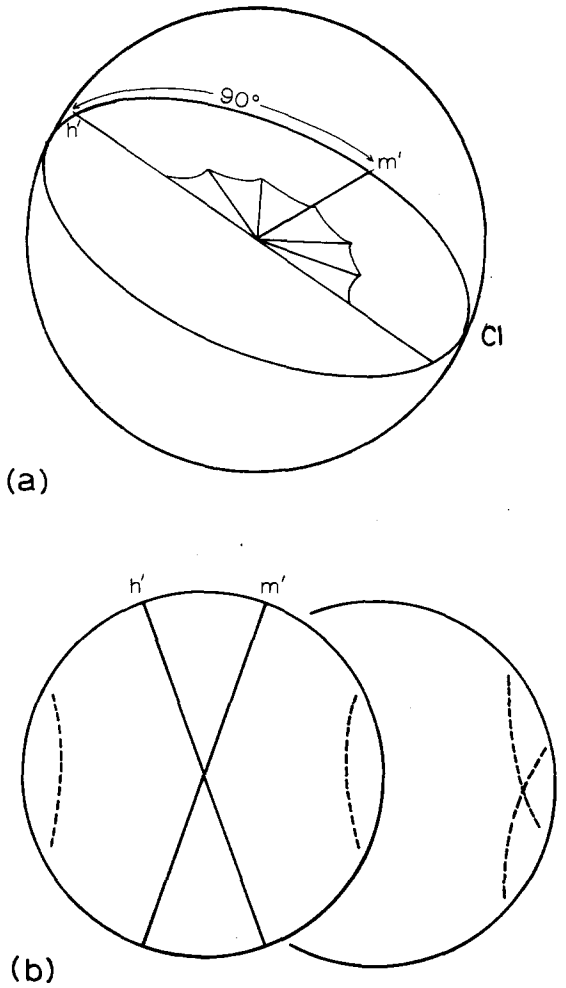

Fig. 6. (a) Orthographic construction for a deformed brachiopod. h', m' are the deformed hinge and median directions. (b) Construction of loci of poles to great circles representing all possible strain ellipses when the principal directions are not independently determined. When two homogeneously deformed specimens are analyzed, their loci intersect at a single point. Similar construction may be made for any bilaterally symmetric fossils.

possible principal direction ϕ_s. As a simple way of representing this (R_s, ϕ_s) locus use the pole to each great circle (plotted on either hemisphere, Fig. 6b). When a fossil symmetry line is chosen as the principal direction, the locus touches the perimeter as infinite unstraining is then required to restore perpendicularity. If a direction in the obtuse angle between symmetry lines is chosen, no real solution is possible, because it is impossible to enlarge an initial right-angle if it contains the maximum principal stretch direction. If two or more specimens are available, their (R_s, ϕ_s) loci may be superimposed as in Fig. 6(b), yielding a unique solution.

Three-dimensional analysis is more complicated because the particle paths are complex space curves, but pure flattening, plane strain and pure constriction are tractable. The construction for flattening is identical to Fig. 4 except that the plane of no distortion (cleavage) is a plane of dilation and is not necessarily horizontal. For constriction, the movement paths are in the reversed sense. The case of plane strain leads to exceedingly complicated constructions and is best tackled numerically (De Paor, in preparation).

Exercise 5: Simple shear of bilaterally symmetric fossils

There is little point in dealing with simple shear in two dimensions. Trilobites are unlikely to be found lined up perpendicular to the boundaries of shear zones! I therefore proceed directly to the three-dimensional situation.

(i) Let A, B, C be reference axes chosen so that C is the pole to a shear zone, B is the zone's monoclinic symmetry axis and A is the displacement direction (Fig. 7). Orientate the net axis parallel to B and trace the fossil's symmetry lines S_1' and S_2'.

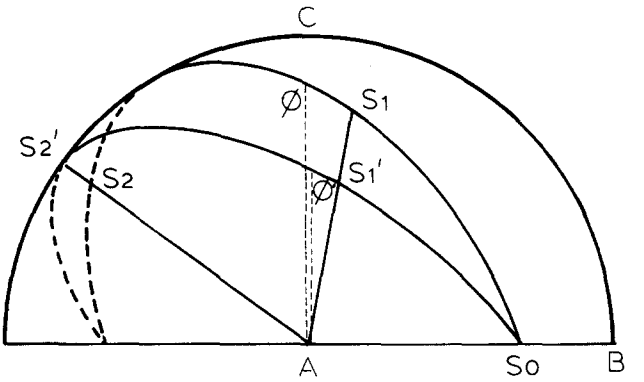

Fig. 7. Three-dimensional simple shear of a bilaterally symmetric fossil. C, pole to shear zone; B, shear axis; A, tectonic transport direction. S_1, S_1', S_2, S_2', fossil's initial and deformed lines of symmetry. S_0, intersection of fossil plane and shear plane. ϕ, ϕ', plunges of lines of intersection of AC plane and fossil plane before and after strain. See text.

(ii) Since all particle paths for simple shear are parallel to the projection lines of Fig. 7, the net may be thought of as a simultaneous projection of the initial unit sphere and each cumulative strain ellipsoid. All displacement vectors are perpendicular to the plane of the figure and all line orientations converge upon A along radial great circles. Therefore the next step is to trace two lines from A through the points representing the attitudes of the symmetry lines, S_1' and S_2'. The initial attitudes of the two lines must lie on these radii. The final constraint upon initial fossil geometry is now enforced.

(iii) Trace the fossil plane through S_1' and S_2' and note its intersection point S_0 on the slip plane AB. The line S_0 suffers no stretch or rotation during deformation, so the initial fossil plane must also contain S_0.

(iv) By rotating the net under the tracing paper, inspect all the great circles that pass through S_0 until one is found to intersect the radii through S_1' and S_2' in a pitch angle of 90°. This, if it is unique, is the undeformed fossil plane.

(v) Note the plunges ϕ and ϕ' of the lines where the initial and final fossil planes pass through the AC plane. Substituting these angles in Fisher's formula,

$$\text{Cot } \phi' = \gamma + \text{Cot } \phi \qquad (3)$$

yields the shear strain γ.

Note the conditional phrase in step (iv) above. There may be cases where two great circles satisfy the criteria

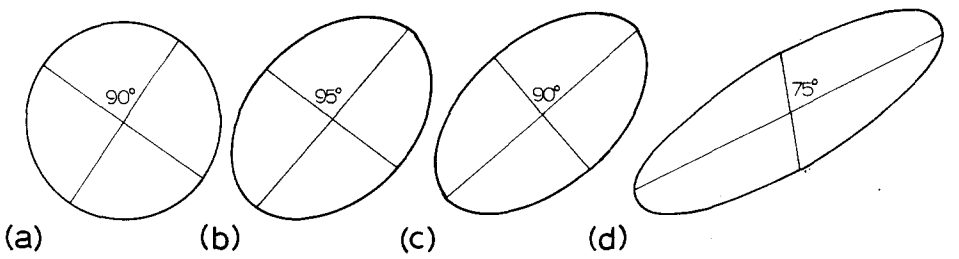

Fig. 8. Illustration of potential ambiguity in the determination of shear strain using only one fossil. Labels are as in Fig. 7, but for simplicity, the fossil is drawn in the AC plane. (a) Undeformed specimen. (b) First increment of deformation. (c) Second increment of deformation restores symmetry. (d) Third increment destroys symmetry, which may be restored by returning either to (a) or to (c).

in this case. To understand the source of this ambiguity, consider the hypothetical two-dimensional case in Fig. 8. Begin with a fossil lying in the AC plane and apply three pulses of simple shear deformation. After the first (Fig. 8b), the fossil's symmetry is destroyed and there is only one way of restoring it. After the second strain increment (Fig. 8c) the fossil's symmetry returns. The initial and final symmetry lines now represent the right stretch and left stretch axes of the simple shear deformation. After the third strain increment the fossil's symmetry is again destroyed. Here is where the ambiguity arises, for it is clearly possible to restore symmetry by returning to the stage in Fig. 8(a) or 8(c). These stages both satisfy the symmetry requirements but differ in aspect ratio of the restored fossil. An identical argument applies to all three-dimensional sections. A second differently oriented specimen will remove this ambiguity as only one value of γ can be a simultaneous solution for the two specimens.

Having uniquely determined the amount of simple shear, the stretches along the symmetry lines are obtained from the ratios of lengths AS_1'/AS_1 and AS_2'/AS_2.

Often it will be possible to define the boundaries of a shear zone but not the displacement direction A. In that event a locus of (γ, A) parameters may be constructed by repeating the above exercise for all possible A directions. Simultaneous solution of such loci for two or more specimens may yield a unique (γ, A) pair.

Exercise 6: Angular strain rosettes

The angle between the initial symmetry lines in all of the cases discussed above was 90°. However, a wide variety of fossil strain markers contain features with some other initial angular relationship. In general, two or more specimens are required for an unambiguous solution. Fossils which permit identification of several angles constitute angular strain rosettes and they often suffice to define both the stretch ratio and principal directions.

Figure 9 shows how to tackle a deformed *Pentacrinus* ossicle, leaf and graptolite (see also Wright & Platt 1982, Ramsay & Huber 1984). In each case inspect the great circles of the net until one is found on which the pitch angles between the deformed fossil features are numerically equal to the initial angles as seen in pristine specimens. The net's axis is either oriented in an independently determined principal direction or on a trial-and-error basis.

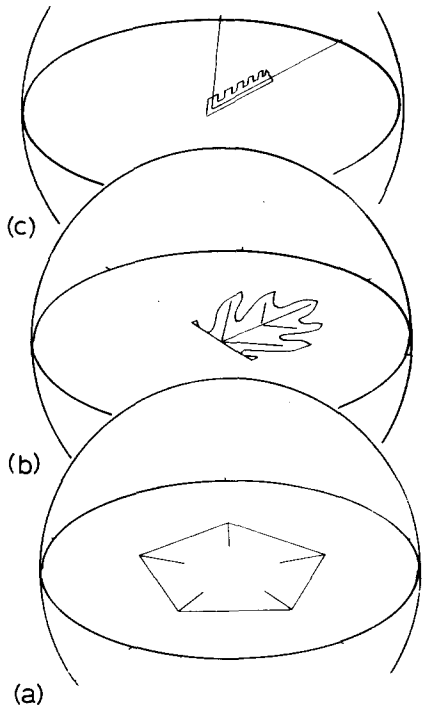

Fig. 9. Non-orthogonal angular strain markers. (a) *Pentacrinus* ossicle. (b) Leaf. (c) Graptolite. See text.

Exercise 7: Folded cross strata

Cross strata are a special type of angular strain marker. They are very important because of their frequent occurrence in the rock record but are problematical because their initial geometry is poorly constrained. The construction in Fig. 10 shows how the initial dip of cross strata may be determined, and the amount of strain calculated under admittedly restricted conditions.

The necessary field situation is shown in Fig. 10(a). Cross strata are exposed on both limbs of a symmetrical fold. Everything other than the foresets is symmetrical about the fold's axial plane. Bedding thickness is essentially constant and the fan angle of cleavage is mirrored

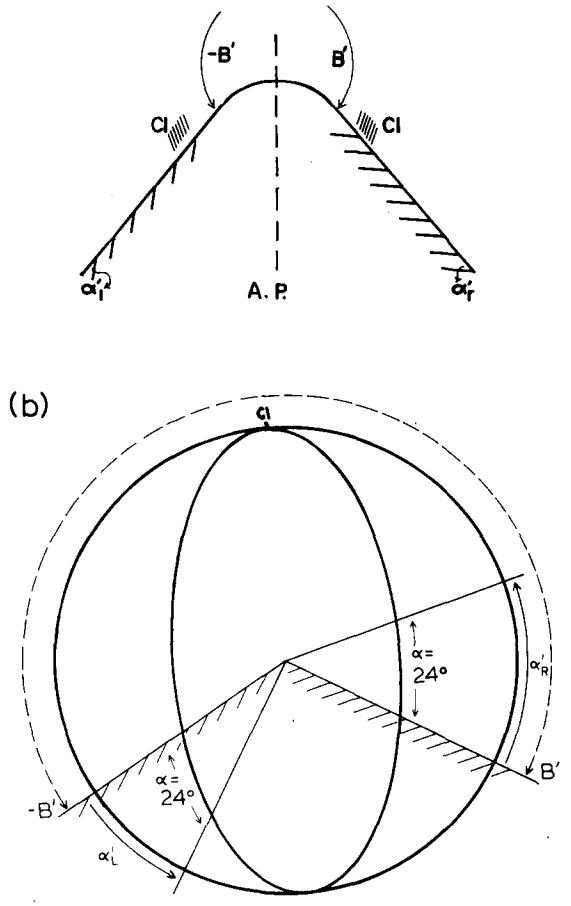

Fig. 10. (a) Deformed cross strata exposed on the limb of a fold which is in every other respect symmetrical about its axial plane. (b) Orthographic construction using the data in (a). *Cl*, cleavage trace; *B'*, angle between cleavage and deformed bedding trace; α, initial foreset angle; α'_L, α'_R, deformed foresets form left and right limbs. See text.

in the axial plane. For a successful strain analysis one need not assume an initial foreset dip angle. It suffices that the angle was initially constant along a single bed and that the two limbs suffered the same intensity of strain.

An orthographic solution is illustrated in Fig. 10(b).

(i) Make a tickmark to represent the cleavage trace. All data from the left limb of the fold are plotted on the left side of the net and all data from the right side of the fold are plotted on the right side of the net; therefore each cleavage trace in turn may be aligned with the tickmark.

(ii) Relative to the cleavage trace, mark the bedding and foreset traces for each limb on the overlay by counting degrees along the perimeter.

(iii) Draw radii of the net to represent the bedding and foreset planes. The cleavage-bedding angles, *B* and *B'*, are equal but opposite because the fold is symmetrical. α'_L and α'_R are set off in the same direction as recorded in the field.

(iv) By rotating the net under the overlay, align the net axis with cleavage trace and inspect the great circles until one is found on which the two bedding-foreset pitch angles are equal (α in Fig. 10b). The common value of this angle is the initial foreset apparent dip and the great circle's axial ratio is the common axial ratio of the strain ellipses from the two limbs (each is presumed to be orientated parallel to the respective cleavage trace in the field).

It should be noted that the foreset trace need not be a true dip line, as long as its apparent dip value was constant across the section before strain.

LONGITUDINAL STRAIN MARKERS

Deformed belemnites have long been used as longitudinal strain markers (e.g. Daubrée 1879) and recently Thakur (1972), Mitra (1976) and Ford & Ferguson (1985) have used tourmaline, rutile and arsenopyrite crystals in similar fashion. Each individual marker differs markedly from its host in ductility, but the total volume of markers is assumed to have an insignificant effect upon bulk strain. The problem is to discover what strain the host would have suffered in the absence of the rigid inclusions.

Exercise 8: Pure shear strain of belemnites or crystals

Given a population of markers subject to the same bulk homogeneous strain, we may estimate the stretches of individual lines using the method of Ferguson (1981), which will not be repeated here. To combine two such stretches and an independent estimate of the principal directions, proceed as follows.

(i) Trace the cleavage or other principal direction indicator on an overlay and align it with the net's axis (Fig. 11).

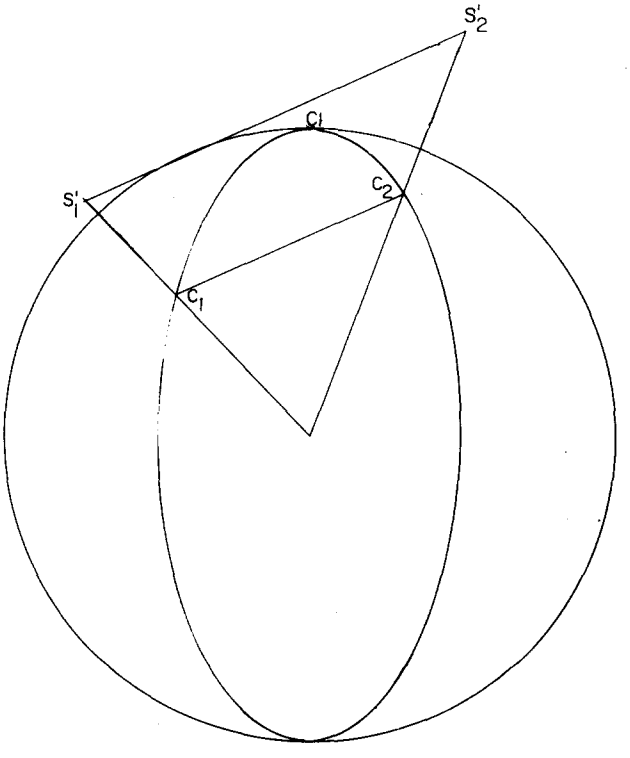

Fig. 11. Orthographic construction for stretched belemnites. S'_1, S'_2, stretches determined from two individuals oriented in the deformed state; C_1, C_2, points where a great circle intersects belemnites in a chord C_1–C_2 which parallels their join S'_1–S'_2. See text.

(ii) Draw vectors S_1' and S_2' radiating out from the centre, parallel to each marker and equal in length to the marker's stretch (the net's radius is taken as unity).

(iii) Join S_1' and S_2' and inspect the great circles of the net until one is found to intersect the vectors in a chord C_1–C_2 which parallels S_1'–S_2'. This great circle has the shape but not the size of the strain ellipse.

(iv) Finally calculate the scaling factor S_1'/C_1 required to convert the stretch ratio given by the chosen great circle into absolute principal stretches.

As before, a minimum stretch ratio and locus of possible intensities and orientations may be plotted in the absence of a cleavage trace and the loci for three specimens taken in pairs may be superimposed. Note that no assumption about marker orientation is necessary (this is fortunate since belemnites are not constrained to die at right angles to one another). An advantage of longitudinal over angular strain markers is that absolute stretches may be recorded. However, two disadvantages should be borne in mind. First, rigid markers will record extension by boudinage only after they enter the field of extension and fibre loading has accumulated to breaking point. Thus they may not contain a complete record of strain. Second, while some pressure-solution shortening may occur in certain rocks, most markers will rotate rigidly while in the field of shortening. Thus the final locus of initially random markers will not lie on a true ellipse but will outline a partial ellipse and partial circle resembling a silhouette of Saturn (N. Fry, pers. comm.).

Exercise 9: Simple shear of belemnites or crystals

A single boudinaged marker in a simple-shear zone may suffice to define the amount of shear strain γ. The necessary construction is illustrated in Fig. 12.

(i) As for other simple-shear constructions, align the net with its axis horizontal and let it represent the direction of the shear zone's monoclinic symmetry axis B. Thus the displacement direction A coincides with the centre pin.

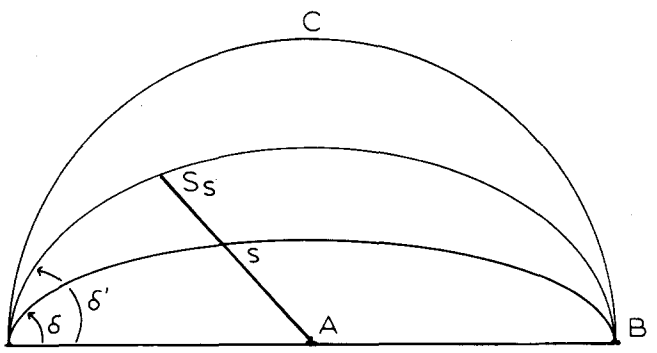

Fig. 12. Construction for a single belemnite subject to simple shear. The fossil is represented by a stereovector, S_s, magnitude point; s, orientation point; δ, initial plane of B axis and fossil; δ', equivalent final plane. See text.

(ii) Use a stereovector (De Paor 1979) to represent the stretch and orientation of the marker. To do this, plot its orientation as a plunge and trend in the conventional way; let this orientation point be a distance s from the origin. Plot a second point along the same radius of the net at distance S_s from the centre pin, where S_s is the marker stretch.

(iii) Draw two great circles through the points s and S_s, meeting in B and note the dihedral angles δ' and δ they make with the AB plane.

(iv) Insert the dihedral angles δ' and δ in Fisher's formula (eqn. 2) to yield the shear strain γ.

In theory the solution is again ambiguous for the plane containing B and the initial marker in Fig. 12 could have been drawn on either the front or back hemisphere. However, in practice, it is not possible for a nearly rigid object to behave homogeneously during its passage through the field of shortening. If it had originated on the back hemisphere it would have rotated rigidly towards the BC plane before stretching. Therefore any markers whose stereovectors touch the perimeter of the net should be interpreted as minimum strain markers which may not have recorded an early history of passage through the shortening field, but any marker whose stereovector falls short of the perimeter may be assumed to have resided in the field of extension from the commencement of strain.

Exercise 10: Cleavage as a strain marker

It is common to use cleavage as an indication of one principal plane of the left stretch component of deformation. However if cleavage is developed in a shear zone, its orientation can be used to estimate strain intensity. If an independent strain marker such as a deflected dyke is present then volume change may be detected.

First consider a zone of simple shear cutting through an undeformed host. Figure 13(a) illustrates the relationship between amount of shear strain γ and orientation of cleavage V. The zone boundary is a direction of no longitudinal strain (i.e. it lies in a circular section in three dimensions). The second line of no longitudinal strain must subtend, at the C axis, an angle ω whose tangent is $\frac{1}{2}\gamma$. This is necessary in order that a shear strain of $-\gamma$ should return the line to an initial attitude $-\omega$ while restoring its initial length. Cleavage must bisect the circular sections, therefore

$$\gamma = 2 * \text{Tan}\ (90° - 2V), \qquad (4)$$

(see Treagus 1981).

Now consider Fig. 13(b), in which the AC-plane trace of a dyke is shown at 130° to the zone boundary outside the shear zone and 80° inside. Cleavage is absent in the host rock and is oriented at $V = 20°$ in the shear zone. To factorize the zone strain into volume loss and simple shear components,

(i) Plot axes A and C and let B coincide with the centre pin (Fig. 13c).

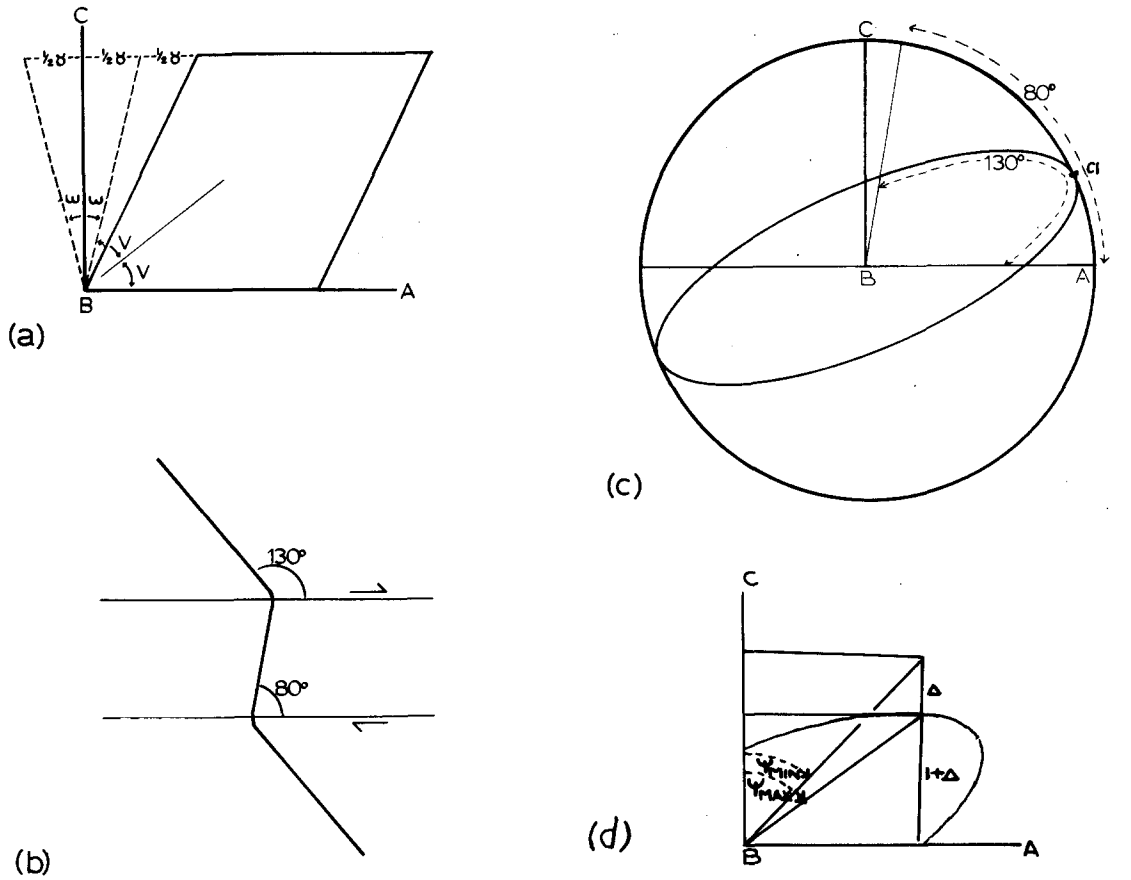

Fig. 13. Strain factorization given a dyke which traverses a shear zone in undeformed host rock. V marks the cleavage direction in the zone. ψ_{min}, ψ_{max} are the range of possible angular shears, depending on strain path. Δ is the percentage compaction. (a) Explanation of eqn. (4). (b) Trace of dyke at 130° to the zone externally and 80° internally. (c) Orthographic construction; net axis is aligned with cleavage trace. (d) Range of possible angular shear values is defined by the rectangle shown. See text for details.

(ii) Align the net axis with cleavage trace, at 20° to A, and draw a line parallel to the deformed dyke direction at 80° to A.

(iii) Inspect the great circles of the net until one is found to subtend an angle of 130° between A and the deformed dyke line.

(iv) Note the ratio of the great circle's height parallel to C to its radius parallel to A (Fig. 13d) and call this ratio $1 + \Delta$.

(v) Restore the initial height of the shear zone by extending the deformed height a distance $-\Delta$. Now the angular shear ψ may be read from Fig. 13(d). Its value is path dependent but must fall between the extremes indicated, representing shear followed by volume loss and volume loss followed by shear. Naturally, the true value of ψ is expected to be intermediate between these extremes, assuming simultaneous shear and volume loss.

Of course, one may object to the use of cleavage as a principal direction indicator in the above circumstances, but the exercise serves as a simple illustration of the power of orthographic analysis in the factorization of deformation. Complicated constructions for superposition of pure and simple shear will usually be more appropriate in practice but are left to the interested reader to work out.

RECONSTRUCTION OF THE THREE-DIMENSIONAL STRAIN ELLIPSOID

A number of the exercises discussed above yielded the three-dimensional deformation ellipsoid or at least its irrotational component, the left stretch ellipsoid. However, others are essentially two-dimensional and present the user with the problem of reconstructing the strain ellipsoid in three dimensions from sectional data (I will continue to use the casual term strain ellipsoid for what is strictly the left stretch ellipsoid). Ramsay (1967) and Milton (1980) have discussed algebraic solutions to this problem, using reciprocal quadratic tensors to represent strain ellipses and their parent strain ellipsoid. A major drawback of the tensor approach is that small errors in tensor components may cause large errors in the orientation of the calculated strain axes (Fig. 14). Here I adopt an alternative approach that does not employ such tensors.

The problem of constructing an ellipsoid to fit three sectional ellipses must be tackled in three stages as errors may render sections incompatible. Only after closing such errors may one proceed to locate the axes of the strain ellipsoid and, finally, its axial ratios.

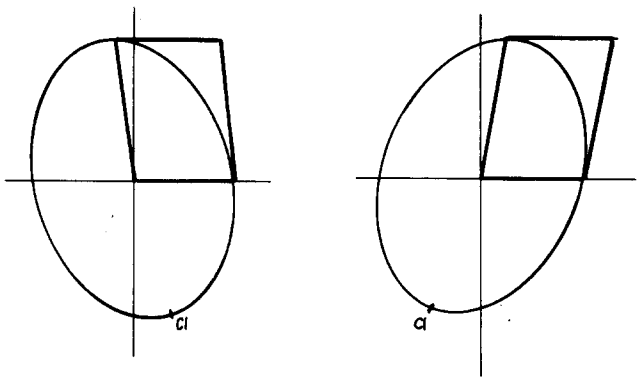

Fig. 14. Illustration of the potentially large effect upon principal directions when tensor components change very little. Only one off-diagonal component has been changed between the left and right hand tensors, yet their ellipses are very differently oriented.

Exercise 11: To render three elliptical sections compatible

Let the triclinic axes *A–B–C* define three planes through a rock (orthogonal axes are perfectly acceptable but not necessary).

(i) Using a single overlay of the orthonet (Fig. 15a), draw lines *OA*, *OB*, *OC*, *OA'* such that the angles $\angle AOB$, $\angle BOC$ and $\angle COA'$ represent the interaxial angles of the three-dimensional reference frame. (Fold the paper until *OA* and *OA'* are parallel as in Fig. 15(b) to check the three dimensional configuration of axes).

(ii) In each sector *AOB*, *BOC* and *COA'*, use the orthonet to draw a portion of the calculated strain ellipse. Note that a pair of ellipses cuts each reference axis; therefore there are two ambiguous estimates of the stretch along each axis. Arbitrary choices of scale on the three section planes may be responsible for some of the ambiguity but it is usually impossible to form a closed loop of elliptical sections by adjustments of scale alone. It is as if the sections represented the boundaries of a spinnaker sail with rips at the axes (Fig. 15b). However, scaling may be used to distribute the errors among the three axes and personal judgement may dictate at this stage whether greater confidence in one strain estimate than another is appropriate. For simplicity, assume that the stretches along *OA* and *OA'* are exactly the same and that all errors arose from the strain estimate in the *BOC* sector. Therefore one need only adjust one ellipse to eliminate all ambiguity. The reader may repeat this procedure on all three sections if desired, closing half of the 'rip' on each axis through correction of each of the two juxtaposed ellipses.

(iii) Draw an error bar on axes *OB* and *OC* as illustrated in Fig. 16(a). Label the ends of the error bars *BB'* and *CC'*, where *B*, *C* are the stretches as determined without error on the *AOB* and *COA* planes and *B'*, *C'* are the corresponding erroneous estimates from the *BOC* plane.

The problem is to adjust the ellipse in the *BOC* sector so that its perimeter passes through points *B* and *C*, not *B'* and *C'*. Three adjustments are possible. Rotating the

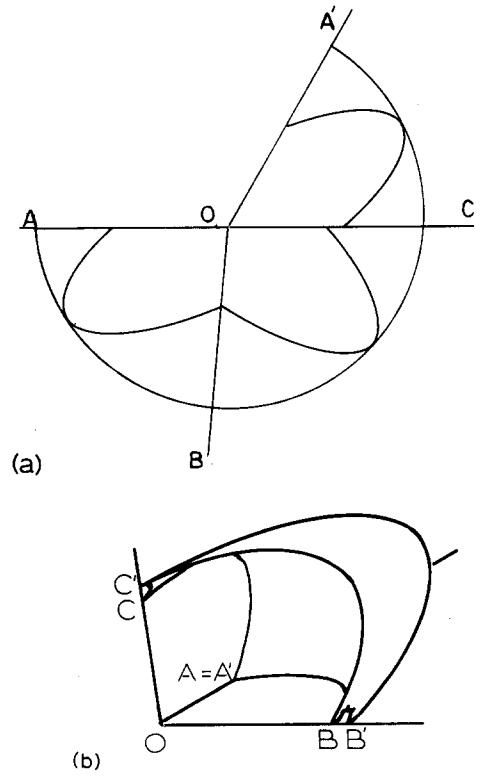

Fig. 15. General triclinic reference fram *A–B–C*. (a) Plane divided into sectors representing the three reference planes in (b). 'Rip' at the reference axes implies incompatibility of strain data. See text.

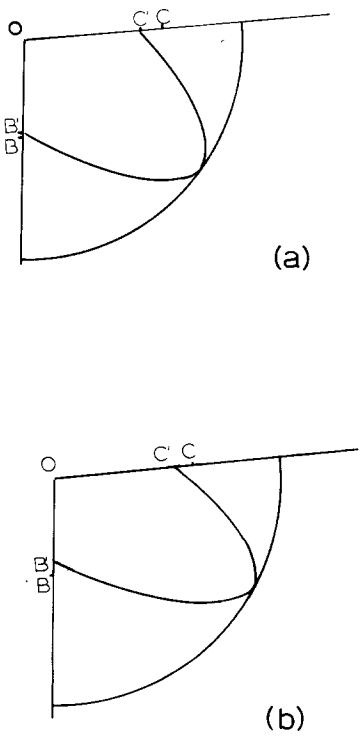

Fig. 16. Closing the errors on axes *B* and *C*. (a) Error bars *BB'* and *CC'*: Note that the calculated ellipse passes through *B'* and *C'*. (b) Ellipse orientation corrected so that eqn. (5) holds.

net and tracing the ellipse with the same axial ratio but slightly different orientation will cause points B' and C' to move in opposite directions along their respective axes. Choosing an ellipse of slightly different axial ratio but unchanged orientation will cause the points B' and C' to migrate in the same direction, whether outwards or inwards. Changing the size but not the shape of the ellipse will also close the error bars simultaneously and since this adjustment does not usually reflect any change in the given data (axial ratios are usually given, not absolute stretches) it is preferable to adjust size rather than shape. Indeed, unnecessary drafting is avoided if one considers errors eliminated as soon as the pairs of stretch estimates OB, OB' and OC, OC' are in the same proportion (Fig. 16b). Therefore, the next step is:

(iv) Adjust the orientation but not the axial ratio of the ellipse in sector BOC until it intersects the reference axes in points B', C' such that

$$OB/OB' = OC/OC'. \quad (5)$$

Now the three ellipse axial ratios and orientations are compatible.

(v) Finally, the stretch of every radius of the corrected BOC sectional ellipse is brought into compatibility with the other two sections by a scaling of OB/OB'; no 'rip' remains in the 'spinnaker sail'.

Exercise 12: To determine the principal directions from three compatible sectional ellipses

This exercise is based on the Biot–Fresnel construction. First it is necessary to determine the circular sections of the strain ellipsoid.

(i) Mark a geographical reference frame such as north-east-down on an overlay of the orthonet and trace three great circles to represent the planes AOB, BOC and COA from the previous example in their correct spatial attitude.

(ii) Using data corrected in the case of the BOC plane, plot the calculated principal directions of the sectional ellipses.

(iii) Mark points at 10° intervals along the three great circles and write beside each tickmark, the corresponding stretch (Fig. 17a). Step (v) of Exercise 11 must be carried out to render absolute stretches from the three planes compatible.

(iv) Inspect the great circles of the net until two are found to intersect the three section planes in points of equal stretch value. These are the circular sections. The inspection procedure may take some time as great circles of all possible dips and all possible strikes must be considered. However, once one circular section is found, the second quickly follows.

The principal directions are now constrained to lie along the intersection of the circular sections and along the bisectors of their dihedral angles (Fig. 17a).

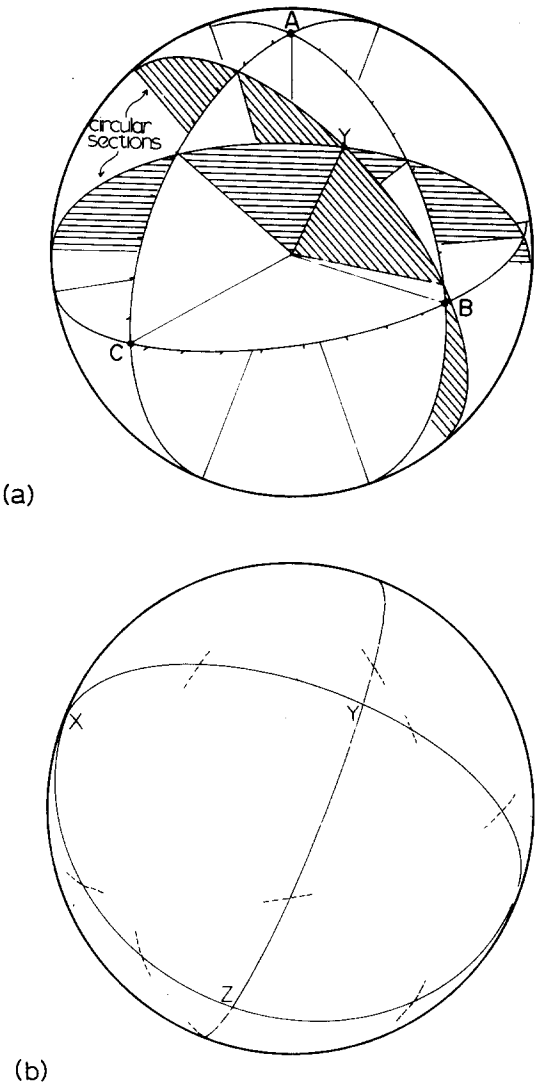

Fig. 17. (a) Determination of the circular sections of the strain ellipsoid using the Biot–Fresnel construction. (b) Determination of three stretches where each principal plane cuts each section plane. See text.

Exercise 13: To determine the principal stretch ratios

Having obtained the principal directions from Exercise 12, it is a simple matter to determine the principle stretch ratios R_{xy} and R_{yz}. Simply note the stretches along the lines where the principal planes XY and YZ cut the section planes (Fig. 17b). For each principal plane there are three such stretches which may be analyzed using the technique previously described for stretched belemnites.

INCORPORATION OF STRAIN DATA IN STRUCTURAL SECTIONS

It is fashionable to draw cross sections through fold belts using principles of retrodeformability (see the review by Suppe 1985). Two assumptions commonly employed are (a) that the rocks underwent plane strain,

with no change of area in the section plane and (b) that bed lengths were conserved during folding. These may be acceptable rules for particular situations but are unacceptable in general; it is usually important to incorporate all available strain data in the structural section. Apparently, it has not been realized that the stretched length of a hangingwall ramp and the deformed cut-off angle of hangingwall beds compared to their undeformed footwall counterparts constitute strain markers as useful as belemnites or brachiopods. The problem is that all such strain readings are inevitably isolated; one must interpolate values between data points before undeforming the section.

Exercise 14: To interpolate strain values between data points

Figure 18(a) shows a section in which strain data are available at three neighbouring points *A*, *B* and *C*. We require an estimate of the strain state at an arbitrary intermediate point *P*.

(i) First, trace the great circles representing the known strain ellipses at *A*, *B* and *C* and plot the pole to each (Fig. 16b: either upper or lower hemispheres may be used, but not a mixture).

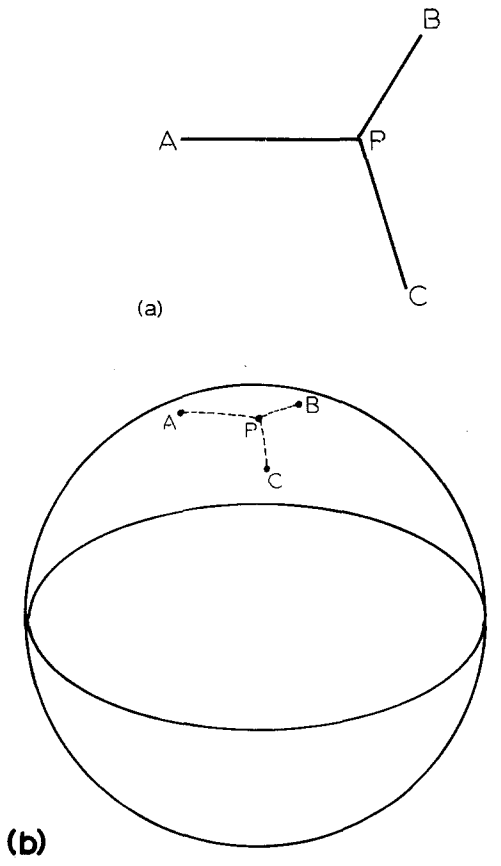

Fig. 18. (a) Three neighbouring strain data points *A*, *B*, *C*. The strain at *P* is to be interpolated. (b) Orthographic construction. Poles *A*, *B*, *C* represent corresponding strain ellipses. Great-circle arcs between pole *P* and *A*, *B*, *C* are in the same proportion as the corresponding distances *PA*, *PB*, *PC* on the outcrop.

(ii) Next locate a pole *P* which subtends angles *PA*, *PB* and *PC* on the net in proportion to the distances *PA*, *PB* and *PC* on the outcrop.

(iii) Finally find the great circle of pole *P* and read its axial ratio and orientation.

Note that only the axial ratio of the interpolated great circle is significant; all great circles have unit long axes, therefore absolute values are not interpretable. Also it is important to realise that the interpolation is non-linear. Principle directions and stretch ratios vary smoothly in all directions, but their rate of change is not constant. In practice, strain measurement errors are so large that there is little point in using a more mathematically refined approach; it is far more important that interpolated values be weighted using personal judgement based on outcrop features.

Exercise 15: To balance a section by undeforming bedlength

The balancing of structural cross sections by conservation of bedlength may yield an acceptable restoration of competent units where outer-arc extension was roughly compensated by inner-arc shortening along the trace of each folded layer. In general, however, beds do not maintain constant length during folding and large errors may result from such simplistic assumptions. Given a dense set of interpolated strain data, we may determine the layer-parallel shortening at every point along a fold profile.

(i) Trace a great circle to represent each principal stretch ratio along the arc of a folded layer. Draw a line on a second overlay to represent the trace of bedding.

(ii) For each ellipse in turn, rotate the second overlay until the trace of bedding makes an angle with the ellipse axis corresponding to that extant on the section.

(iii) Measure the layer-parallel radius of the ellipse as a fraction of the net's radius, multiply it by the maximum principal stretch to yield the actual layer-parallel stretch and by the arc-length over which the reading is presumed to reign.

(iv) Add to the template of undeformed layers a line equal to the undeformed bed-length as calculated in step (iii) and repeat the process for the next arc of bedding.

Exercise 16: To restore the initial area of a section

In the previous exercise we modified the bed-length balancing technique to accommodate layer-parallel strain data. There remains the problem of area change during deformation. Small-scale structures such as stylolites and veins abound in thrust belts and clearly demonstrate mobility of significant volumes of rock constituents. What is not clearly seen in a field examination is the influence of non-plane strain upon the area of a section. The effect of veining can be removed simply by skipping vein material when estimating bed lengths and areas. However, if no attempt is made to account for material lost through pressure solution then it is prob-

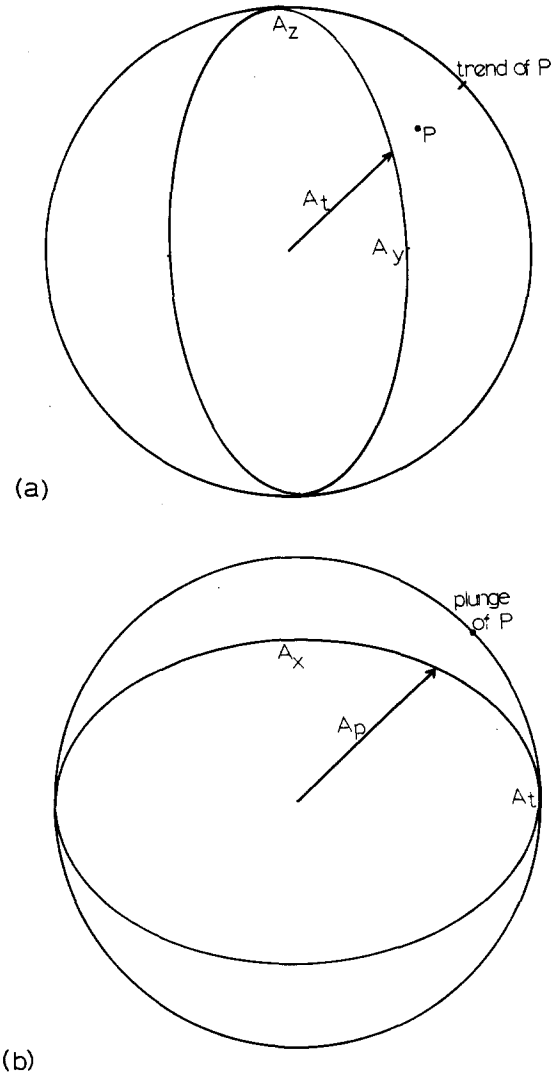

Fig. 19. Balancing a section by restoring its initial area. See text for details.

ably better to include veins in the hope that they roughly balance stylolites.

To estimate the effect of non-plane strain requires more work, but we neglect this factor at our peril. Most strain studies suggest that slaty cleavage forms in strain regimes for which Flinn's parameter k is less than unity (Ramsay 1967). So everywhere we see the trace of cleavage in deformed sections we know that the section plane has lost area even if volume has been preserved in three dimensions. To restore such area loss the area stretch ellipsoid is employed as defined in Part I (De Paor 1983, p. 263). Remember that the term area stretch is used to denote the final area of an initial unit area, as opposed to area strain which refers to the change in an initial unit of area. The principal values of the area stretch ellipsoid are

$$A_x = YZ$$
$$A_y = ZX \quad \text{(De Paor 1983, eqn. 26)}$$
$$A_z = XY.$$

Given the principal area stretches at a particular point on a section, we wish now to calculate the area stretch for the plane of section. Since the plane of section is known in the deformed state, its area stretch is the radius of the area stretch ellipsoid which parallels the pole to the section plane (Fig. 19a). The following procedure locates that radius vector in three dimensions (not to be confused with the two-dimensional construction of Part I, fig. 14 which yielded the area stretch of a plane given its initial pre-deformational pole),

(i) Prepare an orthographic construction for the A_z–A_y principal section of the area stretch ellipsoid and plot the pole to the section plane in its correct relative orientation (Fig. 19b).

(ii) Measure the radius A_t of the area stretch ellipse in the direction of azimuth of the pole in the A_z–A_y–A_x reference frame.

(iii) Prepare a second area stretch construction using A_t and A_x as axes (Fig. 19b) and find the area stretch vector whose inclination is the same as the inclination of the pole in Fig. 19(a). Measure the length of this vector as a fraction of the radius of the net and multiply by A_t to yield the area stretch vector along the section pole, A_p.

(iv) Multiply the area stretch factor A_p by the area over which the given strain reading is considered to reign and append the resultant area to the initial section template.

Repetition of the above procedure for each strain locality on a section need not be laborious especially if the orientation net rotations and tensor calculations are programmed on a digital computer; the reward is a section which is truly retrodeformed, not merely restored using assumptions of bed-length or area conservation that are appropriate only in limited circumstances.

CONCLUSION

The orthographic method, described in theory in Part I (De Paor 1983) and in practice in this paper, represents a unified approach to strain analysis. It is not necessary to commit to memory a vast array of strain techniques. Rather it is sufficient to remember the rule presented above, namely that there is a simple and direct relationship between the strain suffered by an object and the viewpoint from which it appears undeformed to an observer. The orthonet serves to help the geologist decide what is an undeformed view by providing scales of degrees of pitch along great circles which correspond to true angular scales along the perimeter in the undeformed state. Thus, using the orthonet we may measure angles on the deformed objects as if they were in their initial pristine condition. Other nets cannot be used in this fashion because they distort such angles. Only the orthonet conserves vector and tensor operations, and homogeneous strain is one such operation. The net's main drawback is that it is of fixed size, but even this can be overcome with the aid of a microcomputer.

The full power of orthographic analysis is realized when the net is used simultaneously in two different

capacities, both as an orientation net for the analysis of dips, strikes, pitches, plunges and trends, and as a strain net for the measurement of ellipse axial ratios. Such combined usage facilitates three-dimensional strain studies that have no obvious algebraic solution and highlights the errors associated with individual variables in a way that traditional strain studies fail to do. In this author's opinion, the orthonet is potentially as useful in strain analysis as the stereonet is in structural analysis.

Acknowledgements—I thank University College Galway, Université de Rennes, University of Manchester, University of Cardiff, S.U.N.Y. Albany and University of California at Berkeley, Santa Cruz and Los Angeles for hosting 'orthographic workshops' of three- to twelve-hour duration and acknowledge financial support from T.S.G., C.N.R.S., The Fulbright Commission, S.U.N.Y. Albany, U.C. Berkeley, U.C. Santa Cruz, U.C.L.A., Texaco and The Atlantic Richfield Corporation. Celia Kohn assisted with the drafting of figures.

REFERENCES

Borradaile, G. 1973. Curves for the determination of compaction using deformed cross-bedding. *J. Sedim. Petrol.* **43**, 1160.

Cloos, E. 1947. Oolite deformation in the South Mountain Fold, Maryland. *Bull. geol. Soc. Am.* **58**, 843–918.

Cloos, E. 1971. *Microtectonics*. Johns Hopkins University Press, Baltimore.

Daubrée, G. A. 1879. *Études synthetique de geologie experimentale*. Dunod, Paris, 418–422.

De Paor, D. G. 1979. The use of stereovectors in structural and engineering geology. *Tectonophysics* **60**, T1–T6.

De Paor, D. G. 1981a. Strain analysis using deformed line distributions. *Tectonophysics* **73**, T9–T14.

De Paor, D. G. 1981b. A new technique of strain analysis using three dimensional distributions of passively deformed linear markers. *Tectonophysics* **76**, T13–T16.

De Paor, D. G. 1981c. Geological Strain Analysis. Unpublished Ph.D. thesis, National University of Ireland.

De Paor, D. G. 1983. Orthographic analysis of geological structures—I. Deformation theory. *J. Struct. Geol.* **5**, 255–277.

Ferguson, C. C. 1981. A strain reversal method for estimating extension from fragmented rigid inclusions. *Tectonophysics* **79**, T43–T52.

Flinn, D. 1962. On folding during three-dimensional progressive deformation. *Q. Jl. geol. Soc. Lond.* **118**, 385–428.

Ford, M. & Ferguson, C. C. 1985. Cleavage strain in the Variscan Fold Belt, County Cork, Ireland, estimated from stretched arsenopyrite rosettes. *J. Struct. Geol.* **7**, 217–223.

Fry, N. 1979. Density distribution techniques and strained length methods for determination of finite strains. *J. Struct. Geol.* **1**, 221–229.

Hossack, J. R. 1978. The correction of stratigraphic sections for tectonic finite strain in the Bygdin area, Norway. *J. geol. Soc. Lond.* **135**, 229–241.

Means, W. D. 1976. *Stress and Strain*. Springer, New York.

Milton, N. J. 1980. Determination of the strain ellipsoid from measurements on any three sections. *Tectonophysics* **64**, T19–T28.

Mitra, S. 1976. A quantitative study of deformation mechanisms and finite strain in quartzites. *Contr. Mineral. Petrol.* **59**, 203–226.

Ramsay, J. G. 1967. *Folding and Fracturing of Rocks*. McGraw-Hill, New York.

Ramsay, J. G. & Huber, M. I. 1983. *The Techniques of Modern Structural Geology, Vol. 1: Strain Analysis*. Academic Press, New York.

Sanderson, D. J. 1974. Patterns of boudinage and apparent stretching lineation developed in folded rocks. *J. Geol.* **82**, 651–661.

Sanderson, D. J. 1976. The determination of compactional strains using quasi-cylindrical objects. *Tectonophysics* **30**, T25–T32.

Suppe, J. 1985. *Principles of Structural Geology*. Prentice-Hall, New Jersey.

Tan, B. K. 1973. Determination of strain ellipses from deformed ammonoids. *Tectonophysics* **16**, 89–101.

Thakur, V. C. 1972. Computation of the values of the finite strains in the Molare region, Ticino, Switzerland, using stretched tourmaline crystals. *Geol. Mag.* **109**, 445–450.

Treagus, S. H. 1981. A simple shear construction from Thompson & Tait (1867). *J. Struct. Geol.* **3**, 291–293.

Wright, T. O. & Platt, L. B. 1982. Pressure dissolution and cleavage in the Martinsburg shale. *Am. J. Sci.* **282**, 122–135.